8CUEE CONFERENCE PROCEEDINGS
8th International Conference on Urban Earthquake Engineering
March 7-8, 2011, Tokyo Institute of Technology, Tokyo, Japan

THE TSUNAMI VULNERABILITY ASSESSMENT IN PERU USING THE INDEX OF POTENTIAL TSUNAMI EXPOSURE

Hideaki Yanagisawa[1], Koshimura Shunichi[2], Yuji Yagi[3], Yushiro Fujii[4], Gaku Shoji[5], and Cesar Jimenez[6]

1) Tokyo electric power services co., ltd., Japan
2) Associate Professor, Department of Civil Engineering, Tohoku University, Japan
3) Associate professor, Department of Life and Environmental Sciences, University of Tsukuba, Japan
4) International Institute of Seismology and Earthquake Engineering, Japan
5) Associate professor, Department of Engineering Mechanics and Energy, University of Tsukuba, Japan
6) Directorate of Hydrography and Navigation, Peru

h-yanagi@tepsco.co.jp, koshimura@tsunami2.civil.tohoku.ac.jp, yagi-y@geol.tsukuba.ac.jp, fujii@kenken.go.jp, gshoji@kz.tsukuba.ac.jp, cesarsud86@hotmail.com

Abstract: Tsunami vulnerability assessment along the coast of Peru was carried out based on the modeling of the 2001 Camana tsunami. We first conducted field survey of the 2001 Canama tsunami to measure tsunami flow depth and topography of the Camana coast. Based on the field observation, we found that 1 - 3 m of tsunami flow depth inundated the Camana coast and caused significant damage on houses. We then modeled the 2001 Camana tsunami using nonlinear shallow-water theory to examine the validation of a tsunami modeling. As a result, our numerical model is consistent with measured data. Developing the tsunami hazard scenarios, we examined potential tsunami hazard in Peruvian coast using the probability of potential tsunami exposure. Consequently, we found that Lima and Callao face a high risk of major tsunami disaster.

1. INTRODUCTION

Peruvian coast is one of the most important seismologic regions in the world. In the Peru-Chile border region, the largest earthquakes with moment magnitude close to 9.0 occurred in 1604, 1868 and 1877. In recent years, large earthquakes with moment magnitude more than 8.0 occurred in 2001 and 2007. These earthquakes have accompanied large tsunamis which were responsible for extensive property and human damage in Peruvian coast. To develop the effective countermeasure against the tsunamis, the area prone to be tsunami damage should be determined considering tsunami hazards, population and frequency of earthquakes. The purpose of this study is to provide vulnerability assessment to possible tsunami damage for the coastal area of Peru.

According to Koshimura et al.,(2009), tsunami hydrodynamic feature such as tsunami height is greatly related to damage ratio of human or buildings. Therefore, the accurate estimation of tsunami hazards is much required to conduct tsunami vulnerability assessment. We thus estimate tsunami hazards using numerical simulation to determine the detail of tsunami hydraulic feature. We first conduct the modeling of 2001 Camana tsunami to validate the numerical model. We then conduct vulnerability assessment developing tsunami hazard scenarios using population data, the fragility function of human damage and the computed tsunami hazards.

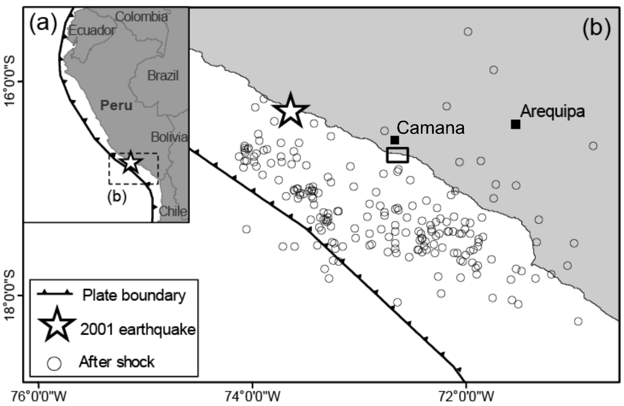

Figure 1 Map of southern coast of Peru showing the epicenter and after shocks of 2001 earthquake. The survey area is shown in the solid line.

2. FIELD SURVEY OF 2001 CAMANA TSUNAMI

2.1 Study area

On June 2001, a major earthquake of moment magnitude 8.4 generated a destructive tsunami that hit the southern coast of Peru (Fig. 1). The tsunami killed at least 25 people with additional 62 missing in the Camana area (Jaffe et al., 2003). Tsunami runup height around Camana area were estimated to have been approximately 3 - 8 m and the tsunami inundation distance extended more than 1 km inland from coast (Okal et al., 2002). Nine years after the tsunami damage, some destroyed houses have been left derelict in the coast of Camana city, which was once the developed beach resort area. To find the evidence of 2001 tsunami, we conducted field investigation at the coast of Camana city.

2.2 Results of field survey

Although 9 years have passed since the tsunami impact, water marks of the tsunami have been remained on walls of some damaged houses. Figure 2 shows the tsunami flow depth inferred from the water marks on damaged houses and witness of the tsunami. The tsunami flow depth is the measuring water depth above the ground. These results show that 1.6 – 3.1 m tsunami inundated the beach resort area. The residential area on flat land stretches approximately 0.3－1.0 km inland so that the tsunami could have easily inundated the overall flat area and caused significant damage to houses (Fig. 2). We also found the trace of damage on the foundation of the house caused by tsunami wave erosion, which is mostly the same as it was when the tsunami attacked (Fig. 3). From field observation 9 years after the tsunami damage in Camana, we found valid data to estimate the tsunami flow.

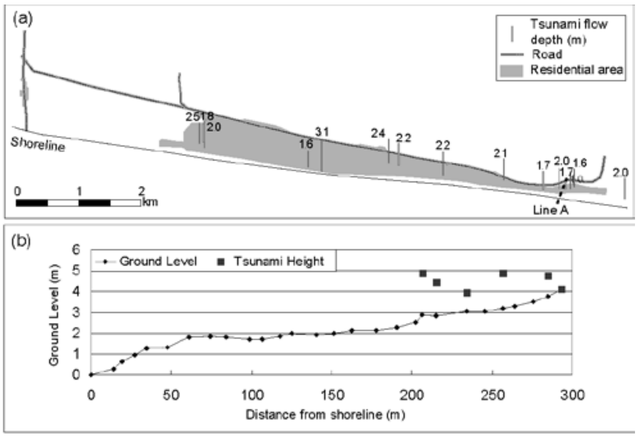

Figure 2 (a) Tsunami flow depth at the coast of Camana city (b) Cross-section view of the ground level with the tsunami heights along the Line A

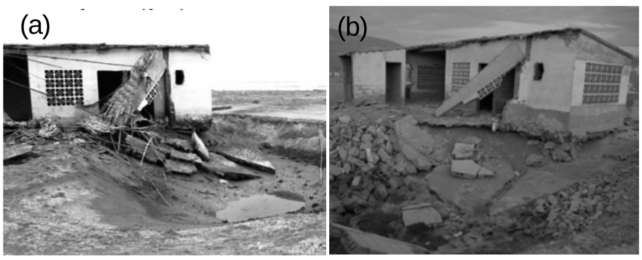

Figure 3 Damaged house and destruction of the foundation in (a) 2001 (Dengler, 2001) and (b) 2010

3. NUMERICAL MODELING OF 2001 CAMANA TSUNAMI

3.1 Fault parameter

The 2001 earthquake ruptured a portion of the plate boundary between the Pacific and Nazca Plates. According to Harvard CMT catalog, the magnitude of 2001 earthquake is estimated to be *Mw*8.4 ($M_0 = 4.67 \times 10^{21} N/m$). To determine the fault length and width, we applied the empirical relationships between moment magnitude *Mw*, fault length *L* and width *W* obtained by Papazachos et al (2004) as equation (1) and (2).

$$Log(L) = 0.5Mw - 2.19 \quad (1)$$
$$Log(W) = 0.31Mw - 0.63 \quad (2)$$

Using the fault area *A* (=*L*×*W*) and scalar moment M_0, the fault displacement *D* is determined by equation (3).

$$M_0 = \mu DA \quad (3)$$

where μ is the rigidity. Table 1 shows the determined fault parameters for 2001 earthquake. We applied the fault depth, angle of strike, dip and slip acquired by Harvard University. For the initial conditions of the tsunami modeling, we estimated the vertical seismic deformation of the land and sea bottom using the theory of Manshinha and Smylie (1971). We assumed instantaneous displacement of the sea surface identical to the vertical seafloor displacement.

3.2 Modeling of tsunami propagation and inundation

To validate a tsunami modeling, we performed numerical simulation of the 2001 Camana tsunami. Tsunami propagation in coastal areas was simulated based on the nonlinear shallow-water theory, which includes the bottom friction in the form of Manning's formula. For tsunami modeling, we made 1350 m grid digital bathymetry/topography data, interpolated from the data provided by the General Bathymetry Chart of the Oceans (GEBCO) Digital Atlas. In addition to GEBCO, we compiled local bathymetric/topography data of southern Peru provided by Directorate of Hydrography and Navigation (DHN), Shuttle Radar Topography Mission (SRTM) data and our measured data to construct merged bathymetry/topography data. The grid size varies from 1350 m to 50 m, constructing a nested grid system.

We compared measured tsunami runup heights with computed values. The local tsunami runup height is the result of measuring the water marks above the astronomical tide level when the tsunami arrived. According to Okal et al. (2002) and this study, totally 25 points of local tsunami

Table 1 Fault parameters for the 2001 Camana tsunami

Mw	Origin of the fault (°)		Length	Width	Dislocation	Dip	Slip	Strike	Depth
	Latitude	Longitude	(km)	(km)	(m)	(°)	(°)	(°)	(km)
8.4	-18.40	-72.30	260	95	4.1	18	63	310	29.6

runup height and inundation flow depth were obtained in the study area. The inundation flow depth (above ground level) is changed to the tsunami runup height using the compiled topography data acquired by this study. The validation of the model is performed by K and κ proposed by Aida (1978) as equations (4), (5) and (6).

$$\log K = \frac{1}{n}\sum_{i=1}^{n}\log K_i \tag{4}$$

$$\log \kappa = \sqrt{\frac{1}{n}\sum_{i=1}^{n}\left(\log K_i\right)^2 - (\log K)^2} \tag{5}$$

$$K_i = R_i / H_i \tag{6}$$

where R_i and H_i are the measured and modeled values of tsunami runup height at point *i*. JSCE (2002) empirically provides the guideline for a tsunami numerical modeling suggesting that $0.95 < K < 1.05$ and $\kappa < 1.45$ as the threshold of valid tsunami source to develop the tsunami hazard assessment.

3.3 Numerical results of 2001 Camana tsunami

To validate our numerical results, we compared measured tsunami runup heights with maximum tsunami runup heights computed from our model. Figure 4 shows the special distribution of the computed maximum tsunami runup height. The tsunami run up averagely 5 meters along the coast of Camana. Figure 5 shows the comparison between measured and computed tsunami runup height. The numerical results were approximately consistent with the measured data, excluding the higher values resulting from water splashing. Our model is sufficiently satisfied with the value of JSCE (2002) (K=0.98, κ=1.34). This finding confirms that our numerical model can be used with confidence to develop the tsunami hazard scenarios.

4. VULNERABILITY ASSESSMENT IN PERUVIAN COAST

4.1 Development of tsunami hazard scenario

During the past 430 years, the 11 largest earthquakes (from *Mw* 8.0 to 8.8) with accompanying large tsunamis have occurred along the plate boundary between the Pacific and Nazca Plates near the Peruvian coast (e.g., Dorbath et al., 1990; Kulikov et al., 2005). To estimate tsunami hazards, we assumed 53 earthquake scenarios with *Mw*8.0, 8.2, 8.4, 8.6, 8.8 along the plate boundary (Fig. 6). Based on the modeling of 2001 tsunami, the fault length, width and displacement of each moment magnitude were determined by equations (1), (2) and (3). The remaining parameters were determined using example of 2001 earthquake (table 2). Tsunami propagation was simulated based on the nonlinear shallow-water theory using spherical coordinate system, which includes the bottom friction in the form of Manning's formula. Here, we used 0.5 sec grid digital bathymetry/topography data provided by GEBCO.

To estimate potential human damage, we used the

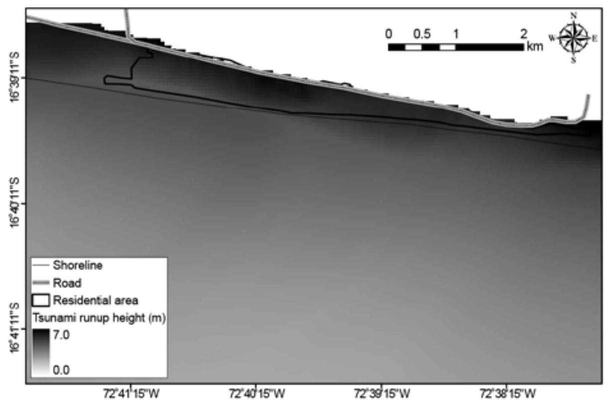

Figure 5 Comparison between measured tsunami runup height and computed maximum tsunami heights. The black outline square presents the higher value resulting from water splashing (Okal et al., 2002)

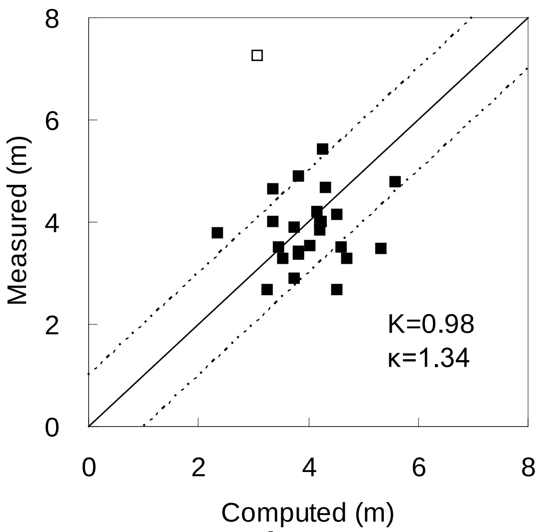

Figure 4 Computed maximum tsunami runup height

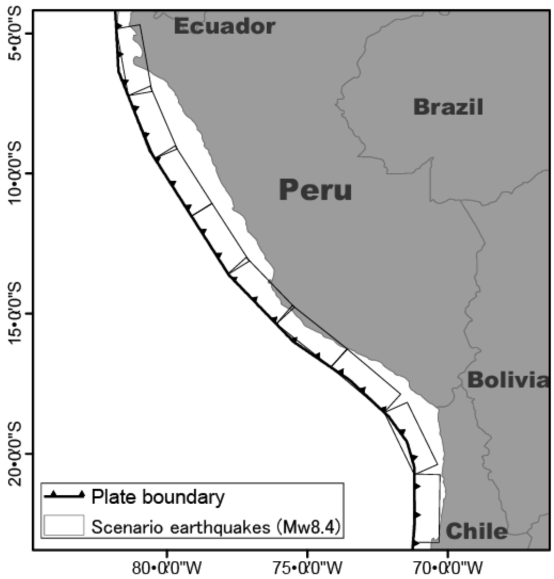

Figure 6 Scenario earthquakes for tsunami vulnerability assessment in the case of *Mw*8.4

following fragility function, which is the relationship between the computed maximum tsunami runup height η and the ratio of human damage $\alpha(\eta)$, which was acquired by the analysis of damage of the 2004 Indian Ocean tsunami (Koshimura et al, 2009).

$$\alpha(\eta) = \Phi[(\eta - \mu)/\sigma] \quad (7)$$

where Φ is the cumulative density function of a standard normal distribution, μ and σ are the mean and standard deviation of η (μ = 5.37, σ = 0.72). Using the Geographic Information System (GIS), we estimated the Potential Tsunami Exposure (*PTE*) multiplying the human damage ratio $\alpha(\eta)$ by global grid population data at shoreline (Ork Ridge National Laboratory, 2006). We further estimate the *t* year probability of exceedance using Poisson process as equation (8),

$$P[PTE \geq a; t] = 1 - \exp(-\lambda t) \quad (8)$$

where $P[PTE \geq a; t]$ is the probability that *PTE* will exceed *a* value at least once in the 50-year, and λ is annual frequency of occurrence. We simply estimated λ by the following equation,

$$\lambda = \sum_{m=1}^{n} \frac{N[PTE \geq a]}{N_m} \times \frac{1}{n} \times \frac{1}{T} \quad (9)$$

where $N[PTE \geq a]$ is the number of scenarios in each magnitude that *PTE* exceeds *a* value, N_m is the number of scenarios in each magnitude, *n* is the number of magnitude (=5) and *T* is the average return period. Here, we assumed that the frequency of occurrence of earthquakes in each magnitude is constant because Peruvian coast is lacking in certain data of the largest earthquakes.

4.2 Results and Discussion

Figure 7 shows the 50 year probability of exceedance when *PTE* will exceed 100 people. This result indicated that the coast of Lima and Callao face a high risk of major tsunami disaster (*P* > 10%). These results provide basic information for the tsunami disaster prevention planning. However, this study is preliminary assessment to detect area prone to be tsunami damage. Thus, additional studies are required to conduct a detailed assessment of the possible tsunami damage in the highest tsunami-risk areas.

Acknowledgements:

The authors acknowledge support from M. Estrada and H. Yanagisawa. This research was supported in part by the JST-JICA project of Science and Technology Research Partnership for Sustainable Development (SATREPS).

Table 2 Fault parameters for scenario earthquakes

Mw	Length (km)	Width (km)	Dislocation (m)	Dip (°)	Slip (°)	Depth (km)
8.0	160	70	2.4	18	90	30
8.2	210	80	3.3	18	90	30
8.4	270	95	4.3	18	90	30
8.6	350	110	5.7	18	90	30
8.8	450	125	7.7	18	90	30

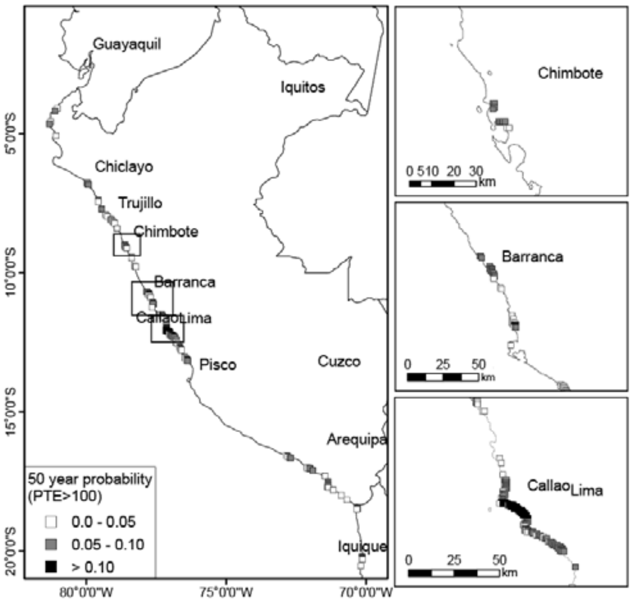

Figure 7 50 year probability of exceedance of Potential tsunami exposure (PTE) along the coast of Peru

References:

Jaffe, B. E., Gelfenbaum, G., Rubin, D. M., Peters, R., Anima, R., Swensson, M., Olcese, D., Anticona, L. B., Gomes, J . C. and Riega, P. C. (2003), "Identification and Interpretation of Tsunami Deposits from the June 23, 2001 Peru Tsunami," *Proceedings of the International Conference on Coastal Sediments 2003*, CD-ROM Published by World Scientific Publishing Corp and East Meets West Productions, Corpus Christi, TX, USA, ISBN 981-238-422-7, 13p.

Kulikov, E. A., Rabinovich, A. B. and Thomson, R. E. (2005), "Estimation of Tsunami Risk for the Coasts of Peru and Northern Chile," Natural Hazards, **35**, 185-209, DOI 10.1007/s11069-004-4809-3.

Okal, E. A., Dengler, L., Araya, S., Borrero, J. C., Gomer, B. M., Koshimura, S., Laos, G., Olcese, D., Modesto, O. F., Swensson, M., Titov, V. V. and Vegas, F. (2002), "Field Survey of the Camana, Peru Tsunami of 23 June 2001, " *Seismological Research Letters*, **73**(6), 907-920.

Papazachos, B. C., Scordilis, E. M., Panagiotopoulos, D. G., Papazachos, C. B. and Karakaisis, G. F. (2004), "Global Relations Between Seismic Fault Parameters and Moment Magnitude of Earthquakes, " *Bulletin of Geological Society of Greece*, vol. XXVI, 1482-1489.

Dorbath, L., Cisternas, A. and Dorbath, C. (1990), "Assessment of the Size of Large and Great Historical Earthquakes in Peru," *Bulletin of the Seismological Society of America*, **80**(3), 551-576.

Aida, I. (1778), "Reliability of A Tsunami Source Model Derived from Fault Parameters," *Journal of Physics of the Earth*, **26**, 73-75.

Manshinha, L. and Smylie, D. E. (1971), "The Displacement Field of Inclined Faults," *Bulletin of the Seismological Society of*

America, **61**, 1433-1440.
Koshimura, S., Namegaya, Y. and Yanagisawa, H. (2009), "Tsunami Fragility - A New Measure to Assess Tsunami Damage, " *Journal of Disaster Research*, **4**(6), 479-488.
Japan Society of Civil Engineers. (2002), "Tsunami Assessment Method for Nuclear Power Plants in Japan, " http://www.jsce.or.jp/committee/ceofnp/Tsunami/eng/JSCE_Tsunami_060519.pdf, 72p.